



Scripta Materialia 59 (2008) 471-474



www.elsevier.com/locate/scriptamat

On the initial microstructure of metallic micropillars

R. Maaß, S. Van Petegem, J. Zimmermann, C.N. Borca and H. Van Swygenhoven*

Paul Scherrer Institute, CH-5232 Villigen, Switzerland

Received 5 April 2008; accepted 20 April 2008 Available online 1 May 2008

White beam Laue microdiffraction has been performed to investigate the initial microstructure of undeformed Au, Ni, Cu, and NiTi micropillars fabricated by focused ion beam milling. Various microstructural features have been shown, from which it is known that they contribute to classical hardening.

© 2008 Acta Materialia Inc. Published by Elsevier Ltd. All rights reserved.

Keywords: Micropillars; Plasticity; Microstructure; Defects; Single crystals

Compression of micron-sized pillars [1] has shown enhanced strengthening in face-centered cubic [2,3] and body-centered cubic [4] single crystals when the pillar diameter is reduced to below 20 µm. From the published mechanical data, however, it is evident that a scatter as high as 100% can exist for nominally identical samples [5,6], which can in part been explained by the stochastic nature of plasticity [7,8]. In these approaches it is assumed that the initial pillar structure does not contain microstructural features classically known to result in hardening and that the pillars are strain-gradient-free single crystals. However, white beam Laue diffraction has demonstrated that this is not always the case: the first example is an Au pillar with a pre-existing strong strain gradient that rules the selection of the slip system [9]; the second is an Ni pillar containing a low-angle grain boundary [10]. Here, we report on the initial microstructure prior to deformation of 14 single crystal and two multi-grained pillars, classified into six groups according to chemical substance and crystallographic orientation. Laue diffraction reveals several microstructural features that within classical crystal plasticity are known to result in hardening, ranging from misorientations at the pillar base to twin defects and in homogeneous strain gradients in the body of the pillars. In two samples containing multiple grains, strain gradients were also found in each of the individual grains.

Table 1 shows the chemical composition, orientation, and diameter of the 16 investigated pillars tabulated into six groups. Most of the pillars were made from the same material as reported in Ref. [10] for Ni, Ref. [11] for Cu,

Ref. [9] for Au $\langle 346 \rangle$, Ref. [12] for NiTi and Ref. [13] for sputtered Au. The Au $\langle 123 \rangle$ samples were made using the same procedure as the Au $\langle 346 \rangle$ samples in Ref. [14]. The initial bulk material was a commercially available single crystal, except for the sputtered Au and the Au $\langle 346 \rangle$. Au $\langle 346 \rangle$ pillars were cut out of larger grains in an annealed foil, as was done in Refs. [9,14]. All samples within each group were made out of the same bulk piece, with a typical pillar-to-pillar distance of 50–100 µm, except the Cu samples, which were focused ion beam (FIB) milled from individual single crystal bulk pieces.

The FIB milling conditions were different between all the sample groups, but the same within each: for instance, final current densities of 50 pA were applied for Au $\langle 123 \rangle$ and Au $\langle 346 \rangle$, 100 pA for the Cu pillars and 1 nA for the Ni pillars, whereas the acceleration voltage was 30 keV in all cases. White beam Laue diffraction was performed in transmission at the MicroXAS beam line of the Swiss Light Source with a microfocused white X-ray beam having an energy distribution ranging from 2 to 22 keV and a beam size between 0.8 and 2 µm in the focal plane. Further details on the experimental technique are given in the online material of Ref. [9]. For each group of pillars a reference Laue pattern of a Si wafer was recorded under the same conditions, which allows monitoring of the resolution function and verification of the calibration parameters.

The range in photon energy used in white beam Laue diffraction allows lattice curvatures and small angular misorientations to be detected without the need for a rocking curve. For instance, excess dislocations of one sign generating a lattice curvature results in a streaked

^{*}Corresponding author. E-mail: helena.vs@psi.ch

Table 1. Sample	groups with	n their	chemical	composition,	vertical	
crystal axis orientation and corresponding pillar diameters						

Group	Chemical composition	Crystallographic orientation	Diameter (µm)
1	Au	⟨123⟩	$3 \times 2.0, 3.0, 4.0$
2	Au	(346)	0.8, 3.0
3	Cu	⟨421⟩	5.0, 5.4
4	Ni	(123)	2×8
5	Ni-50.9 at.%Ti	$\langle 210 \rangle$	2.3, 2.8, 3.0
6	Au	Sputtered (111)	0.9, 1.1

Laue diffraction peak. The angular width of such a streaked peak can then be used to estimate the radius of lattice curvature, which is proportional to the excess dislocation density times the Burgers vector [15,16]. On the other hand, when geometrical necessary dislocations (GNDs) organize into geometrically necessary boundaries (GNBs) to reduce the stored energy, the Laue spot will split, reflecting the contributions from two separate crystal volumes [17]. The above simple approach has been applied to estimate the dislocation densities from the (hkl) reflection showing the largest streak or split, assuming the existence of only one slip system populated with an excess dislocation density.

In several of the investigated samples, misorientations (GNBs) were observed at the pillar base. In the group of the Au $\langle 123 \rangle$ samples, two pillars with a peak split in the lower part were identified by mapping the sample with Laue patterns along its vertical axis. Figure 1a shows a scanning electron microscopy (SEM) image taken under a 66° tilt angle of a 3 µm Au(123) pillar with a height of 8 µm, that is, an aspect ratio of 1:2.7. The Laue diffraction intensity of the (2-2-2) reflection is given in Figure 1b-e for different positions of the incoming X-ray beam along the pillar axis. Note that all experiments are performed in transmission geometry with the incoming beam perpendicular to the pillar axis. At position 4 (Fig. 1e) the Laue pattern corresponds with the single crystal orientation and none of the diffraction peaks show peak splitting. When scanning downwards, the intensity distribution of the Laue peaks evidence a transition from a single diffraction peak towards a split peak at the pillar base, that is, Figure 1c taken at position 2. At position 3, that is more than half-

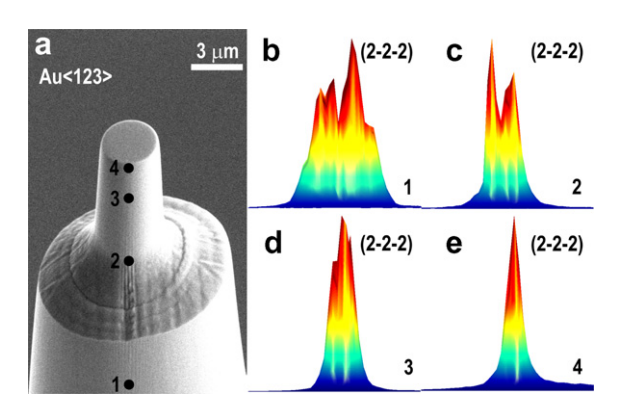


Figure 1. An SEM image of a 3 μ m Au(123) pillar, with split peaks along its vertical axis shown in Figure 2b–e; position 3 is 5 μ m above the pillar–base transition.

way along the pillar length or $5\,\mu m$ above the pillar-base, the smeared out intensities of the overlapping peaks show that the misorientation extends from the base well into the pillar and that only the upper part of the pillar corresponds with a single crystal orientation.

From the splitting of the Laue peaks at position 2 (8 μm from the pillar's top) a misorientation angle of 0.07° is derived, which is equal to a GND density of $\sim 2.8 \times 10^{12} \,\mathrm{m}^{-2}$ in the GNBs present in the probed volume. A similar split was observed in one of the 2 µm Au(123) samples, whereas the other Au pillars of the same group did not exhibit any misorientations at the pillar base. Peak splitting with a magnitude of $0.07^{\circ}/4.9 \times 10^{12} \,\mathrm{m}^{-2}$ was also observed at the base of the 8 µm Ni sample (called Ni B). In particular cases, peak splitting was even observed in the center of the pillar. For example, in the 0.8 μ m Au $\langle 346 \rangle$ pillar and the 2.3 µm NiTi sample, splitting angles and corresponding GND densities of $0.42^{\circ}/2.5 \times 10^{13} \,\mathrm{m}^{-2}$ (Au $\langle 346 \rangle$) and $0.23^{\circ}/1.8 \times 10^{13} \,\mathrm{m}^{-2}$ (NiTi) were found. The intensity distribution of the NiTi $(00\bar{2})$ peak and the Au $\langle 346 \rangle$ $(\bar{2}2\bar{2})$ at half the pillar height are displayed in Figure 2a and b. In addition to the substructure in the 0.8 μm Au(346) pillar, it was found that the pillar itself was rotated relative to the substrate by 0.72°, compared with the vertical axis obtained from fits performed on the entire Laue pattern from the pillar base and taken at half the pillar height. Figure 2b shows that both the substrate and the pillar $(\bar{2}2\bar{2})$ signal are shifted by 0.48° with respect to each other. Due to similar pillar height and beam size, a substrate signal is also recorded at half the pillar height. Note that the pillar and its substrate were machined out of a single grain, which is why the entire pillar is rotated with respect to the orientation of the substrate. Pre-existing GNBs will contribute as a Hall-Petch-like hardening factor according to $\tau_{\rm f} = K(Gb)^{0.5}/(D_{\rm GNB})^{0.5}$, where $\tau_{\rm f}$ is the flow tress, K is a constant, G is the shear modulus, b is the Burgers vector and D_{GNB} is the spacing of the GNBs [18]. Moreover, a misorientation in the lower pillar part will hinder dislocation escape into the base and result in back stresses similar to a decaying stress field under load due to the tapering of the pillar, which also artificially hardens the sample. Misfits at the pillar base complicate the imposed boundary conditions of the compression test and therefore also the comparison of pillars with and without misfits.

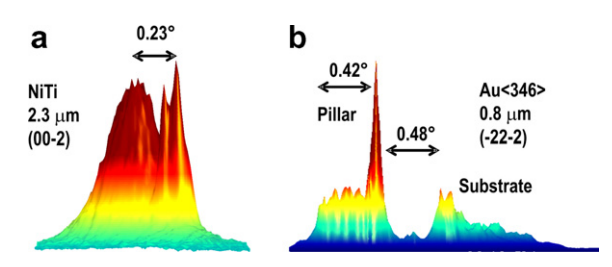


Figure 2. (a) Split (00-2) NiTi peak and (b) split $(\bar{2}2\bar{2})$ Au(346) peak of the 800 nm pillar and a 0.48° misorientation between the pillar and the substrate, which were initially of identical orientation.

Download English Version:

https://daneshyari.com/en/article/1502595

Download Persian Version:

https://daneshyari.com/article/1502595

<u>Daneshyari.com</u>